Soft- and Hard-Agglomerate Aerosols Made at High Temperatures

Stavros Tsantilis and Sotiris E. Pratsinis*

Particle Technology Laboratory, Institute of Process Engineering, Department of Mechanical and Process Engineering (D-MAVT), ETH Zürich, Sonneggstrasse 3, ML F25, CH-8092 Zurich, Switzerland

Received December 17, 2003. In Final Form: April 19, 2004

Criteria for aerosol synthesis of soft-agglomerate, hard-agglomerate, or even nonagglomerate particles are developed on the basis of particle sintering and coalescence. Agglomerate (or aggregate) particles are held together by weak, physical van der Waals forces (soft agglomerates) or by stronger chemical or sintering bonds (hard agglomerates). Accounting for simultaneous gas phase chemical reaction, coagulation, and sintering during the formation and growth of silica (SiO_2) nanoparticles by silicon tetrachloride ($SiCl_4$) oxidation and neglecting the spread of particle size distribution, the onset of hard-agglomerate formation is identified at the end of full coalescence, while the onset of soft-agglomerate formation is identified at the end of sintering. Process conditions such as the precursor initial volume fraction, maximum temperature, residence time, and cooling rate are explored, identifying regions for the synthesis of particles with a controlled degree of agglomeration (ratio of collision to primary particle diameters).

Introduction

Nanoparticle commodities such as carbon black, filamentary nickel (Ni), zinc oxide (ZnO), pigmentary titania (TiO_2), and fumed silica (SiO_2) are produced by well-established industrial aerosol processes involving flame, hot-wall, and spray pyrolysis reactors. The control of particle growth during the employed high temperatures and extremely short residence times (usually <1 s) is crucial, as product powder applications depend on particle size distribution, morphology, and degree of agglomeration as well as surface chemistry and phase composition.[1]

More specifically, depending on the process conditions, particles may be held together by weak physical van der Waals forces (soft agglomerates) or by stronger chemical or sintering bonds (hard agglomerates). Soft agglomerates or even nonagglomerated particles are useful in the manufacture of pigments, nanocomposites, porous electrodes, and quantum dots. In contrast, hard agglomerates with open structures and high surface-to-volume ratios are attractive for fillers, light-guide preforms by external deposition, insulating materials, chemical−mechanical polishing agents, and catalyst supports. Knowing and controlling the extent of powder agglomeration is therefore important, as it can minimize the use of postgrinding or other costly secondary separation techniques when limited particle necking is desired. In practice, the distinction between hard and soft agglomerates is largely empirical, as it is related to the required effort to split apart particles prior to or during their processing.

Pratsinis et al.[2] made nonagglomerated titania particles (~90 nm in diameter) by oxidation of $TiCl_4$ in single diffusion flames, as was confirmed by Hyeon-Lee et al.[3] using small-angle X-ray scattering (SAXS). Lehtinen et al.[4] approximated the onset of agglomeration when the characteristic time for coalescence (sintering) (τ_s) exceeded the characteristic time for particle collisions (τ_c). The results from this approach were consistent with the measured primary particle diameters of flame-made nanosized alumina and titania[5] and even niobium oxide.[6] Moreover, Windeler et al.[6] stated that when τ_s increased much faster than τ_c ($d\tau_s/dt \gg d\tau_c/dt$ after $\tau_c = \tau_s$) soft agglomerates of spherical particles were formed, while oblong particles (hard agglomerates) were formed when τ_s increased slightly faster than τ_c ($d\tau_s/dt > d\tau_c/dt$). However, the formation of weakly agglomerated (softly bonded) hard agglomerates was not considered. Windeler et al.[7] produced spherical nonagglomerated niobium oxide (Nb_2O_5) nanoparticles by injecting the appropriate precursor as a free jet into a methane−air flame. Analysis of the transmission electron microscopy (TEM) pictures of titania and especially alumina (Al_2O_3) particles made under the same conditions revealed more agglomerated structures. Weakly agglomerated silica nanoparticles (as indicated by TEM pictures) of ~200 nm in primary particle diameter were also made in diffusion flames when oxygen (instead of air) was used as oxidant.[8] Glumac et al.[9] used a low pressure flame to make loosely agglomerated nanopowders of titania, silica, and alumina with a mean diameter between 10 and 20 nm. Similarly, the TEM pictures of TiO_2 made in premixed flames in the presence of external electric fields showed titania particle structures with limited neck formation.[10]

The morphology of flame-made ceramic particles is related quantitatively to their sintering history in the flame.[11] When such data are coupled with fluid-particle

* To whom correspondence should be addressed. E-mail: pratsinis@ptl.mavt.ethz.ch.

(1) Pratsinis, S. E.; Spicer, P. T. *Chem. Eng. Sci.* **1998**, *53*, 1861.
(2) Pratsinis, S. E.; Zhu, W.; Vemury, S. *Powder Technol.* **1996**, *86*, 87.
(3) Hyeon-Lee, J.; Beaucage, G.; Pratsinis, S. E.; Vemury, S. *Langmuir* **1998**, *14*, 5751.
(4) Lehtinen, K. E. J.; Windeler, R. S.; Friedlander, S. K. *J. Aerosol Sci.* **1996**, *27*, 883.
(5) Xing, Y.; Rosner, D. E. *J. Nanopart. Res.* **1999**, *2*, 277.
(6) Windeler, R. S.; Lehtinen, K. E. J.; Friedlander, S. K. *Aerosol Sci. Technol.* **1997**, *27*, 191.
(7) Windeler, R. S.; Lehtinen, K. E. J.; Friedlander, S. K. *Aerosol Sci. Technol.* **1997**, *27*, 174.
(8) Zhu, W.; Pratsinis, S. E. *AIChE J.* **1997**, *43*, 2657.
(9) Glumac, N. G.; Chen, Y.-J.; Skandan, G.; Kear, B. *Mater. Lett.* **1998**, *34*, 148.
(10) Kammler, H. K.; Pratsinis, S. E.; Morrison, P. W., Jr.; Hemmerling, B. *Combust. Flame* **2002**, *128*, 369.
(11) Koch, W.; Friedlander, S. K. *J. Colloid Interface Sci.* **1990**, *140*, 419.

10.1021/la036389w CCC: $27.50
Published on Web 05/29/2004

dynamics models,[12] it becomes clear that the product particle characteristics (such as size, crystallinity, and morphology) are determined largely by the maximum flame temperature, cooling rate, and precursor concentration in a given reactor.[13,14] Of course, many other parameters beyond the above core ones such as the reactor design,[15] additives,[16] and electric fields[17] can also influence particle characteristics.

Here, quantitative criteria for the synthesis of hard-agglomerated, soft-agglomerated, or even nonagglomerated particles are developed with a simple model accounting for simultaneous chemical reaction, coagulation, and sintering.[18] This model is chosen for its consistency with more elaborate models accounting for detailed particle size distributions[19] as well as its broad use in computational fluid dynamics simulations of flame synthesis of ceramic nanoparticles.[12,20,21] Furthermore, the effects of the key process parameters (such as maximum temperature, residence time, precursor concentration, and cooling rate) on the degree of agglomeration of fumed silica made by oxidation of silicon tetrachloride ($SiCl_4$) are investigated under non-isothermal conditions. Fumed silica is chosen primarily for its diverse applications and the availability of reliable reaction and sintering rate data.

Theory

Silica is formed by chemical reaction, coagulation, and sintering in the absence of a nucleation barrier[22] by oxidation of silicon tetrachloride according to the following overall stoichiometric formula: $SiCl_4(g) + O_2(g) \rightarrow SiO_2(s) + 2Cl_2(g)$. An overall expression for that reaction is[23]

$$\frac{dC_{SiCl_4}}{dt} = -(k_1 C_{SiCl_4} + k_2 C_{SiCl_4} C_{O_2} \rho_g) \qquad (1)$$

where C_{SiCl_4} (mol/g) and C_{O_2} (mol/g) are the concentrations (per grams of gas) of $SiCl_4$ and O_2, respectively, t (s) is the residence time, ρ_g (g/cm^3) $= MW_g P/(RT)$ is the gas mixture density (where MW_g (g/mol) is the molecular weight of the gas mixture (reactant, product, and carrier gases), P (=1 atm) is the pressure, T (K) is the gas temperature, and R is the universal gas constant), k_1 (1/s) $= 1.7 \times 10^{14}$ exp(−48 314/T), and k_2 (cm^3/(mol s)) $= 3.1 \times 10^{19}$ exp(−48 314/T). The first right-hand side (RHS) term of eq 1 represents the thermal decomposition of $SiCl_4$ as a rate-limiting step to the short-lived intermediate $SiCl_3^{\bullet}$ that rapidly reacts with oxygen to produce SiO_2 and Cl_2. This term dominates at modest $O_2/SiCl_4$ ratios (<20), while the second RHS term of eq 1 dominates at a high excess of oxygen ($O_2/SiCl_4 > 20$), accelerating the conversion of $SiCl_4$ to SiO_2.[23] Given the large excess concentrations of O_2 considered here, it is assumed that the rate of formation of SiO_2 is equal to the rate of loss of $SiCl_4$.

A monodisperse model for aerosol coagulation and sintering[18] is employed here to calculate the evolution of the primary (d_p, cm) and collision (d_c, cm) particle diameters as well as that of the total particle number (N, #/g$_{gas}$), surface area (A, cm^2/g$_{gas}$), and volume concentration (V, cm^3/g$_{gas}$) (per mass of carrier gas). This model is further modified to account for the source term of monomer particles by gas phase oxidation of the precursor.[24] In summary, the governing equations are

$$\frac{dN}{dt} = -\frac{dC_{SiCl_4}}{dt} N_A - \frac{1}{2}\beta N^2 \rho_g \qquad (2)$$

where N_A is Avogadro's number and β (cm^3/(s #)) is the collision frequency function for Brownian monodisperse coagulation calculated by the so-called Fuchs interpolation from the free-molecular to the continuum regimes.[18,25] The rates of change of the area and volume particle concentrations are, respectively,

$$\frac{dA}{dt} = -\frac{dC_{SiCl_4}}{dt} N_A \alpha_m - \frac{1}{\tau_s}(A - N\alpha_s) \qquad (3a)$$

and

$$\frac{dV}{dt} = -\frac{dC_{SiCl_4}}{dt} N_A v_m \qquad (3b)$$

where α_s (cm^2) is the surface area of a completely fused (spherical) particle of volume V/N and α_m ($\approx 6.14 \times 10^{-15}$ cm^2) and v_m ($\approx 4.53 \times 10^{-23}$ cm^3) are, respectively, the area and volume of a silica monomer (molecule). The effect of agglomerate structure in β is incorporated by the so-called collision diameter (so that $\beta = f(d_c)$):[18]

$$d_c = \left(\frac{6V}{A}\right)\left(\frac{A^3}{36\pi N V^2}\right)^{1/D_f} = d_p (n_p)^{1/D_f} \qquad (4)$$

where n_p is the average number of primaries per agglomerate and D_f is the mass fractal dimension, here equal to 1.8, which is common for particles generated by cluster−cluster agglomeration.[26] Although D_f may vary during particle sintering and coagulation, as it has been shown by Monte Carlo[27,28] and other[29] simulations, it hardly affects d_p and d_c over the range of the present conditions. In addition, the characteristic time for viscous flow sintering of silica is[24]

$$\tau_s = 6.5 \times 10^{-15} d_p \exp\left(\frac{8.3 \times 10^4}{T}\left(1 - \frac{d_{p,min}}{d_p}\right)\right) \qquad (5)$$

where $d_{p,min} = 1$ nm and $\tau_s \rightarrow 0$ (instantaneous sintering, full coalescence) for $d_p \leq d_{p,min}$. Furthermore, the characteristic collision time (τ_c, s) is[11]

(12) Johannessen, T.; Pratsinis, S. E.; Livbjerg, H. *Chem. Eng. Sci.* **2000**, *55*, 177.
(13) Mühlenweg, H.; Gutsch, A.; Schild, A.; Riest, K.; Becker, C. Simulation for Process and Product Optimization. In *Silica* [CD-ROM]; Vidal, A., Haidar, B., Eds.; ICSI: Mulhouse, France, 2001.
(14) Varga, G. Commercializing Chemical Nanotechnology: Realization of Complete Solutions using Chemical Nanotechnology. Presented at the International Nano Conference Top Nano 21, St. Gallen, Switzerland, Sept. 11, 2003.
(15) Pratsinis, S. E.; Kodas, T.; Dudukovic, M. P.; Friedlander, S. K. *Ind. Eng. Chem. Process Des. Dev.* **1986**, *25*, 634.
(16) Xiong, Y.; Pratsinis, S. E.; Mastrangelo, S. V. R. *J. Colloid Interface Sci.* **1992**, *153*, 106.
(17) Kammler, H. K.; Jossen, R.; Morrison, P. W., Jr.; Pratsinis, S. E.; Beaucage, G. *Powder Technol.* **2003**, *135−136*, 310.
(18) Kruis, F. E.; Kusters, K. A.; Pratsinis, S. E.; Scarlett, B. *Aerosol Sci. Technol.* **1993**, *19*, 514.
(19) Xiong, Y.; Pratsinis, S. E. *J. Aerosol Sci.* **1993**, *24*, 283.
(20) Schild, A.; Gutsch, A.; Muehlenweg, H.; Kerner, D.; Pratsinis, S. E. *J. Nanopart. Res.* **1999**, *1*, 305.
(21) Johannessen, T.; Pratsinis, S. E.; Livbjerg, H. *Powder Technol.* **2001**, *118*, 242.
(22) Ulrich, G. D. *Combust. Sci. Technol.* **1971**, *4*, 47.
(23) Powers, D. R. *J. Am. Ceram. Soc.* **1978**, *61*, 295.
(24) Tsantilis, S.; Briesen, H.; Pratsinis, S. E. *Aerosol Sci. Technol.* **2001**, *34*, 237.
(25) Seinfeld, J. H. *Atmospheric Chemistry and Physics of Air Pollution*; John Wiley & Sons: New York, 1986.
(26) Schaefer, D. W.; Hurd, A. J. *Aerosol Sci. Technol.* **1990**, *12*, 876.
(27) Akhtar, M. K.; Lipscomb, G. G.; Pratsinis, S. E. *Aerosol Sci. Technol.* **1994**, *21*, 83.
(28) Kostoglou, M.; Kostandopoulos, A. G. *J. Aerosol Sci.* **2001**, *32*, 1399.
(29) Artelt, C.; Schmid, H.-J.; Peukert, W. *J. Aerosol Sci.* **2003**, *34*, 511.

$$\tau_c = \frac{2}{\beta N \rho_g} \quad (6)$$

assuming all particle collisions to be successful.

Ordinary differential eqs 1−3 are solved numerically by any method, here using the VODPK[30] solver with an initial time step of 10^{-40} s. The initial (for $t = 0$ s) values of the dependent variables are $C^0_{SiCl_4} = \phi/MW_g$, $C^0_{O_2} = (1 - \phi)/MW_g$, $N^0 = 0$, $A^0 = 0$, and $V^0 = 0$, where ϕ is the initial molar fraction of $SiCl_4$ and for an inlet balance $(1 - \phi)$ that of O_2. To avoid division by zero during numerical integration, N, A, and V are initially set to very small but finite values, the choice of which does not affect the results: $N^0 = 1$, $A^0 = \alpha_m N^0$, and $V^0 = v_m N^0$. Finally, the employed temperature profiles are those of an initial ($t = 0$) linear increase from $T = 300$ K to T_{max} at $t = t_{max}$, followed by a linear decrease at a constant cooling rate (CR, K/s) until $T = 300$ K (Figure 1, solid lines).

Results and Discussion

Distinction between Soft and Hard Agglomerates and Nonagglomerates. Figure 1 shows axial temperature profiles for three different constant cooling rates (CR = 10^2, 10^4, and 10^6 K/s at $t \geq t_{max}$) along with the $SiCl_4$ conversion % for an initial $SiCl_4$ molar fraction of $\phi = 0.01$ and a maximum process temperature of $T_{max} = 2200$ K, reached at $t_{max} = 2$ ms. Here, the precursor is converted completely to SiO_2 when the peak temperature ($t = t_{max} = 2$ ms) is reached. This is also the case for $T_{max} \geq 2200$ K and the initial precursor molar fractions considered in the present study (ranging from $\phi = 0.001$ to $\phi = 0.5$). Achieving high conversion of the precursor (at the end of the process) is important, as it minimizes the secondary treatment of the off-gases (especially when Cl_2 is present) or even the waste of costly chemicals. In general, the above conditions are consistent with those typically encountered in aerosol flame reactors for the synthesis of fumed silica and other ceramic nanoparticles: Maximum flame temperatures on the order of 2000 K are reached after ∼3−4 ms followed by cooling rates ranging from 6000 to 22 000 K/s for the synthesis of TiO_2 by oxidation of titanium tetraisopropoxide.[31] Similar peak temperatures are reached after ∼2 ms followed by an ∼10 000 K/s cooling rate[32] for the synthesis of SiO_2. The total process residence times are on the order of 1 s.[1]

Figure 2a shows the evolution of the silica total particle surface area concentration (A) (dash-dot line) as well as that for full coalescence ($\tau_s \rightarrow 0$) ($A_{coal.}$) (dash-double-dot line) along with the corresponding average primary (solid line) and collision (dashed line) particle diameters for $T_{max} = 2200$ K, $t_{max} = 2$ ms, CR = 10^4 K/s, and $\phi = 0.01$. The total particle area concentration is initially increasing as long as $SiCl_4$ is oxidized, forming new particles. It reaches its maximum at $t = 1.86$ ms, when the gain from the conversion of $SiCl_4$ (89% at that point in Figure 1) exactly equals the loss by sintering (eq 3a). Eventually, when the process residence time is long enough ($t = 30$ ms), A (dash-dot line) attains effectively a constant value (here, within a four-digit accuracy), indicating conditions of "pure" agglomeration where agglomerates are formed by particle collisions without further particle neck formation and growth.[31] In contrast, when full coalescence is assumed

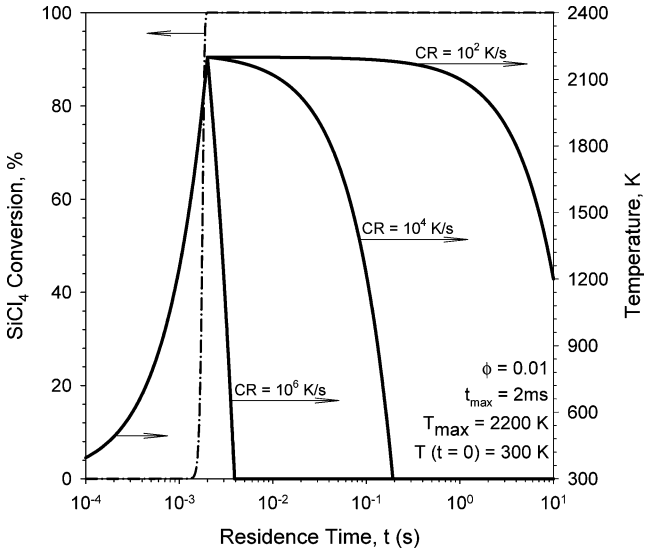

Figure 1. Temperature profiles for a maximum temperature of 2200 K, reached at $t_{max} = 2$ ms, and three different cooling rates (CR = 10^2, 10^4, and 10^6 K/s) along with the $SiCl_4$ % conversion (dot-dashed line) for an initial molar fraction of $\phi = 0.01$ (the $SiCl_4$ conversion profiles for $0.1 \leq \phi \leq 0.001$ are virtually the same).

at all times (dash-double-dot line), the particle area concentration keeps decreasing by coagulation (Figure 2a, $t > 0.007$ s).

The regions of agglomeration can be seen in more detail by tracing the evolution of the primary particle and agglomerate collision diameters. At the early stages of particle formation and growth, $t < 0.0022$ s (Figure 2a, white region), the temperature and precursor conversions increase (Figure 1), and spherical particles form as they fully coalesce upon collision. As a result, the agglomerate collision and primary particle diameters are indistinguishable ($d_c = d_p$), while the characteristic time for coagulation is much larger than that for sintering ($\tau_c \gg \tau_s$), as shown in Figure 2b.[4,5] Later on, at $t > 0.0022$ s, as temperature drops (Figure 1, CR = 10^4 K/s), sintering becomes slower, so τ_s increases faster than τ_c ($t > 0.004$ s) and the particles do not fully coalesce upon collision. As a result, the collision diameter grows faster than the primary particle diameter, reflecting the formation of necks between colliding particles ($d_c > d_p$, $\tau_c \sim \tau_s$ (Figure 2b), and A is not constant). At this stage, firm bonding between colliding particles takes place as the total aerosol area concentration keeps decreasing, indicating the occurrence of coalescence and the formation of hard agglomerates (Figure 2a, 0.0022 s < t < 0.031 s, gray region).

The region of hard agglomerates is bound at small particle sizes by the onset of agglomeration (Figure 2a, open diamond symbol) that is defined at the point where a 1% divergence between the collision and primary particle diameters occurs ($d_c/d_p = 1.01$), similar to the definition of boundary layers. This definition, although arbitrary but unambiguous, is consistent with Windeler et al.,[6] who stated that "oblong" particles are formed when the evolutions of collision and coalescence times are comparable.

The upper boundary of the hard-agglomerate region is set by the formation of soft agglomerates. In more detail, at longer residence times (Figure 2a, $t > 0.031$ s) and even lower process temperatures, sintering effectively stops as $\tau_c \ll \tau_s$ (Figure 2b) and the total aerosol area concentration is essentially constant (Figure 2a). As a result, colliding particles are held together by physical (van der Waals) forces but not chemical or sintering bonds. This indicates the formation of soft agglomerates. When this critical point

(30) Brown, P. N.; Byrne, G. D.; Hindmarsh, A. C. *SIAM J. Sci. Stat. Comput.* **1989**, *10*, 1038.
(31) Tsantilis, S.; Kammler, H. K.; Pratsinis, S. E. *Chem. Eng. Sci.* **2002**, *57*, 2139.
(32) Briesen, H.; Fuhrmann, A.; Pratsinis, S. E. *Chem. Eng. Sci.* **1998**, *53*, 4105.

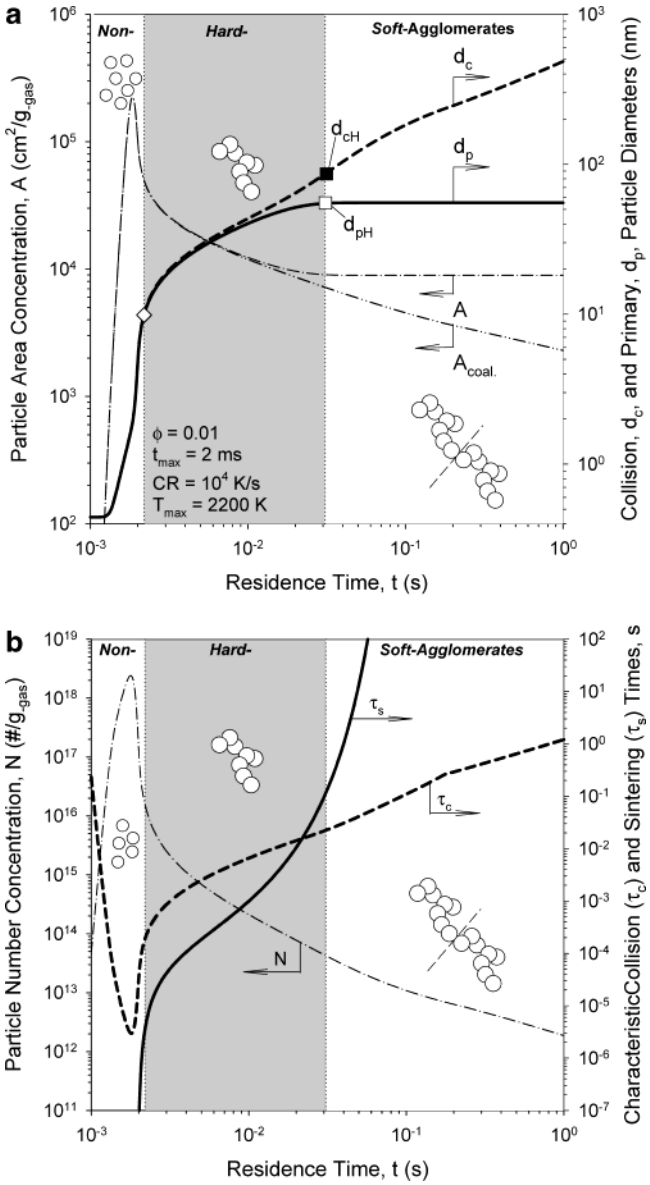

Figure 2. Evolution of silica: (a) total particle area concentration for partial sintering (dash-dot line) and full coalescence (dash-double-dot line) and primary particle (solid line) and agglomerate collision (dashed line) diameters; (b) total particle number concentration (dash-dot line) and characteristic sintering (eq 5, solid line) and collision (eq 6, dashed line) times for $T_{max} = 2200$ K, $t_{max} = 2$ ms, CR = 10^4 K/s, and $\phi = 0.01$. The end of full coalescence is when $d_c/d_p = 1.01$ (part a, open diamond), while the onset of soft-agglomerate formation (part a, open square) is when $d_{pF}/d_p = 1.01$ (or, equivalently, $d_p = d_{pH}$ when d_p reaches $0.99d_{pF}$), d_{pF} being the final constant, within a four-digit accuracy, value of d_p. In part b, the characteristic collision time reaches a minimum at ~2 ms, when the conversion of $SiCl_4$ is complete (Figure 1) and the particle number concentration starts to decrease by the dominance of coagulation.

is reached (Figure 2a, square symbols), primary particle growth is virtually frozen (Figure 2a, solid line plateau, d_p = constant). Similar to the onset of hard-agglomerate formation, the transition from hard to soft agglomerates (Figure 2a, square symbols) is defined as the point at which the average primary particle diameter becomes 99% of its final constant, within a four-digit accuracy, value (d_{pF}) (when $d_{pF}/d_p = 1.01$). For brevity, the particle size characteristics at the end of the hard-agglomerate region will be simply referred to as the hard-primary (d_{pH}) and hard-agglomerate collision (d_{cH}) particle diameters; hence, when $d_p = 0.99d_{pF}$, $d_p = d_{pH}$ and $d_c = d_{cH}$.

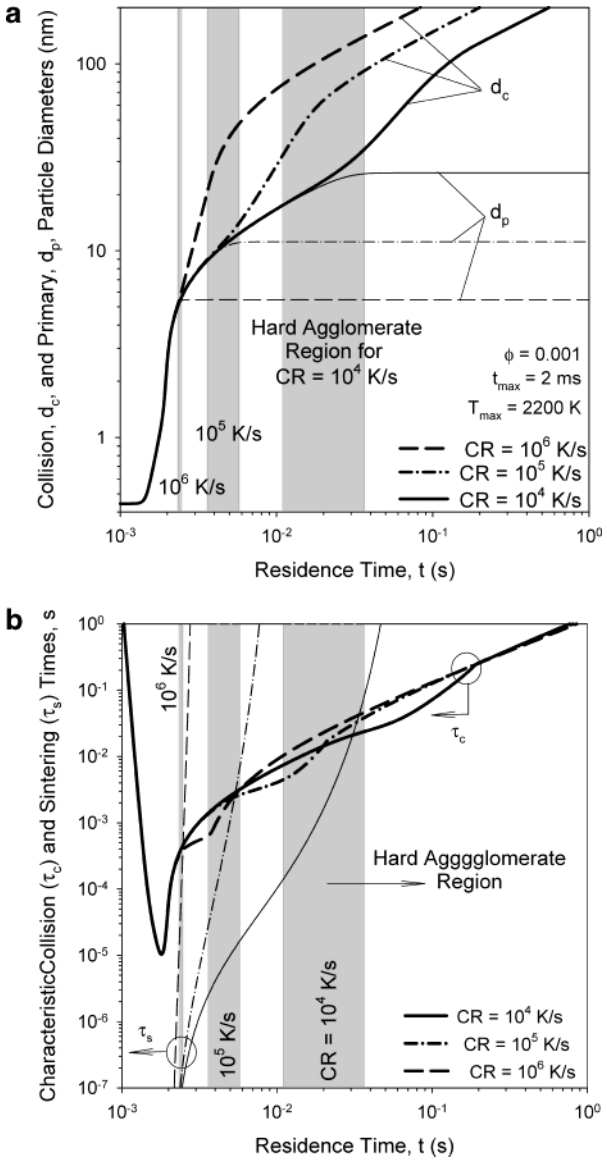

Figure 3. Evolution of silica: (a) primary particle (thin lines) and agglomerate collision (bold lines) diameters; (b) characteristic sintering (thin lines) and collision (bold lines) times for $T_{max} = 2200$ K, $t_{max} = 2$ ms, $\phi = 0.001$, and three different cooling rates (CR = 10^4 K/s (solid lines), 10^5 K/s (dash-dot lines), and 10^6 K/s (dashed lines)). The gray columns represent periods (regions) of formation of hard agglomerates (in reference to Figure 2a). The higher the cooling rate, the broader the angle between the corresponding collision and sintering characteristic times at their intersections (part b).

In the soft-agglomerate region (Figure 2a, $t > 0.03$ s), the degree of agglomeration (d_c/d_p) is increasing constantly, as particle growth is driven solely by coagulation (pure agglomeration). Apparently, at a residence time of 1 s (which is typical in aerosol flame processes), the degree of agglomeration is quite high. Whether these particles consist of single spheres or smaller hard agglomerates depends on the degree of agglomeration at the end of the hard-agglomerate region ($h = d_{cH}/d_{pH}$) where generally each hard agglomerate contains n_p (~h^{D_f}) primary particles, where $D_f = 1.8$ here.

Effect of Process Parameters on the Overall Particle Size Evolution. Figure 3a shows the evolution of the silica average primary (thin lines) and collision (bold lines) particle diameters for $T_{max} = 2200$ K, $t_{max} = 2$ ms, $\phi = 0.001$, and three different cooling rates (CR = 10^4, 10^5, and 10^6 K/s). The three gray columns (from right to left)

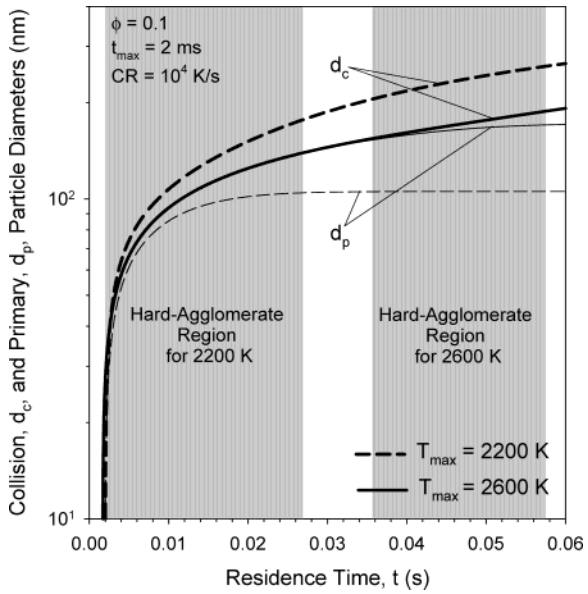

Figure 4. Evolution of silica primary particle (thin lines) and agglomerate collision (bold lines) diameters for CR = 10^4 K/s, t_{max} = 2 ms, ϕ = 0.1, and maximum temperatures of 2200 K (dashed lines) and 2600 K (solid lines).

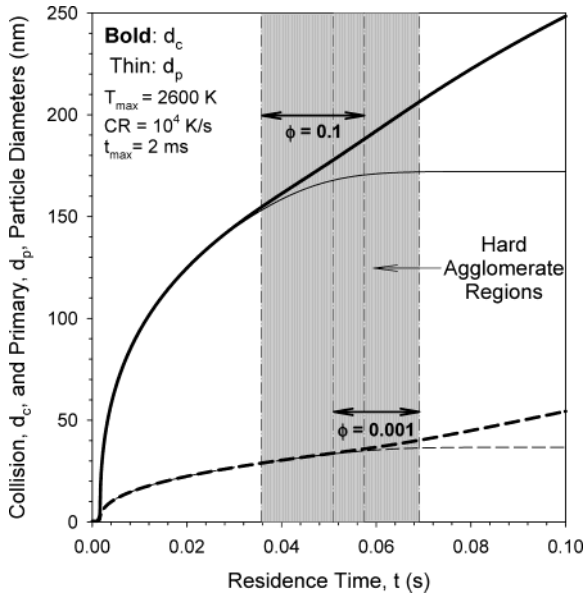

Figure 5. Evolution of silica primary particle (thin lines) and agglomerate collision (bold lines) diameters for T_{max} = 2600 K, t_{max} = 2 ms, CR = 10^4 K/s, and initial $SiCl_4$ molar fractions of 0.001 (dashed lines) and 0.1 (solid lines).

represent the periods (regions) of formation of hard agglomerates (in reference to Figure 2a) for each of these cooling rates. Increasing the cooling rate (by 2 orders of magnitude) shortens the period (region) of hard-agglomerate formation (again roughly by 2 orders of magnitude) and increases the intersection angle between τ_s and τ_c (Figure 3b). For CR = 10^6 K/s, τ_s becomes much larger than τ_c quickly (Figure 3b), while the hard-agglomerate region collapses into a single line (Figure 3a), corresponding to particles essentially free of hard agglomerates ($d_{pH} \approx d_{cH}$ or $h \approx 1$). This is consistent with Windeler et al.,[6] who suggested that loosely (softly) agglomerated spherical particles are formed when $d\tau_s/dt \gg d\tau_c/dt$ at $\tau_s \approx \tau_c$.

As depicted here, the cooling rate is probably one of the most effective ways to control the morphology and size characteristics of hard agglomerates. Cooling of particles

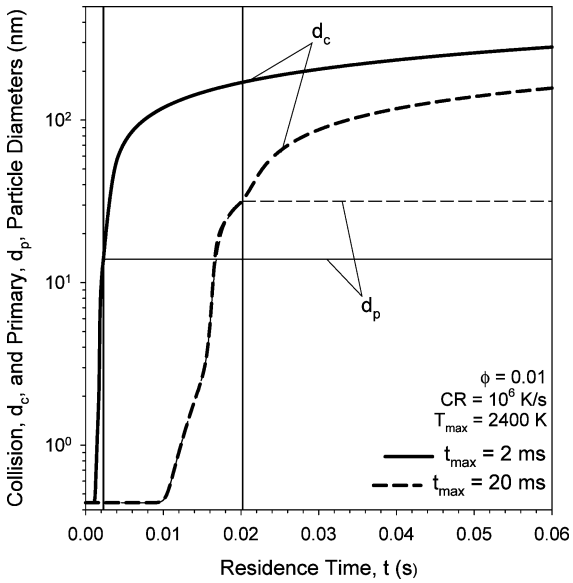

Figure 6. Evolution of silica primary particle (thin lines) and agglomerate collision (bold lines) diameters for CR = 10^6 K/s, ϕ = 0.01, and T_{max} = 2400 K reached at t_{max} = 2 ms (solid lines) and 20 ms (dashed lines).

can be achieved by mixing them with cold gas,[33] by the use of an external nozzle quenching device,[34] or even by an external electric field.[17] In general, increasing the cooling rate hinders sintering and accelerates fractal-like particle coagulation (especially in the free-molecular regime), resulting in bigger collision and smaller primary particle diameters, respectively. On the other hand, when the cooling rate is slow (CR = 10^4 K/s), the divergence between the primary and collision diameters (that manifests the onset of agglomeration, in general) is delayed and less abrupt, indicating longer periods of full coalescence and prolonged hard agglomeration (Figure 3a, widest gray column). Moreover, if the cooling rate is fast enough (to cause, for example, a practically instant decrease to room temperature, as shown in Figure 1 for CR = 10^6 K/s), the upper and lower boundaries of the hard-agglomerate region can collapse into a single point (Figure 3a, the thinnest, linelike, gray column), reflecting the onset of the attainment of soft agglomerates of spherical particles ($h \approx 1$ as $d_{pH} \approx d_{cH}$).

Figure 4 compares the evolution of d_p (thin lines) and d_c (thick lines) at t_{max} = 2 ms, ϕ = 0.1, and CR = 10^4 K/s for two maximum process temperatures, T_{max} = 2200 K (dashed lines) and 2600 K (solid lines). Higher T_{max} values accelerate reaction kinetics and prolong particle coalescence, promoting eventually the formation of larger primary particles but smaller agglomerates. The onset of agglomeration at T_{max} = 2200 K (Figure 4, divergence between the bold and thin dashed lines) occurs at earlier residence times ($t \sim 2$ ms) than those at T_{max} = 2600 K ($t \sim 36$ ms). This trend is in agreement with Zhu and Pratsinis[8] who measured (by nitrogen absorption) bigger silica particles with a lower degree of agglomeration (as indicated by TEM pictures) at higher flame temperatures that were achieved by switching the oxidant from air to oxygen.

Figure 5 shows that increasing the precursor loading from ϕ = 0.001 to ϕ = 0.1 enhances both primary and agglomerate particle growth for T_{max} = 2600 K, t_{max} = 2 ms, and CR = 10^4 K/s. Increasing the precursor concen-

(33) Hansen, J. P.; Jensen, J. R.; Livbjerg, H.; Johannessen, T. *AIChE J.* **2001**, *47*, 2413.
(34) Wegner, K.; Stark, W. J.; Pratsinis, S. E. *Mater. Lett.* **2002**, *55*, 318.

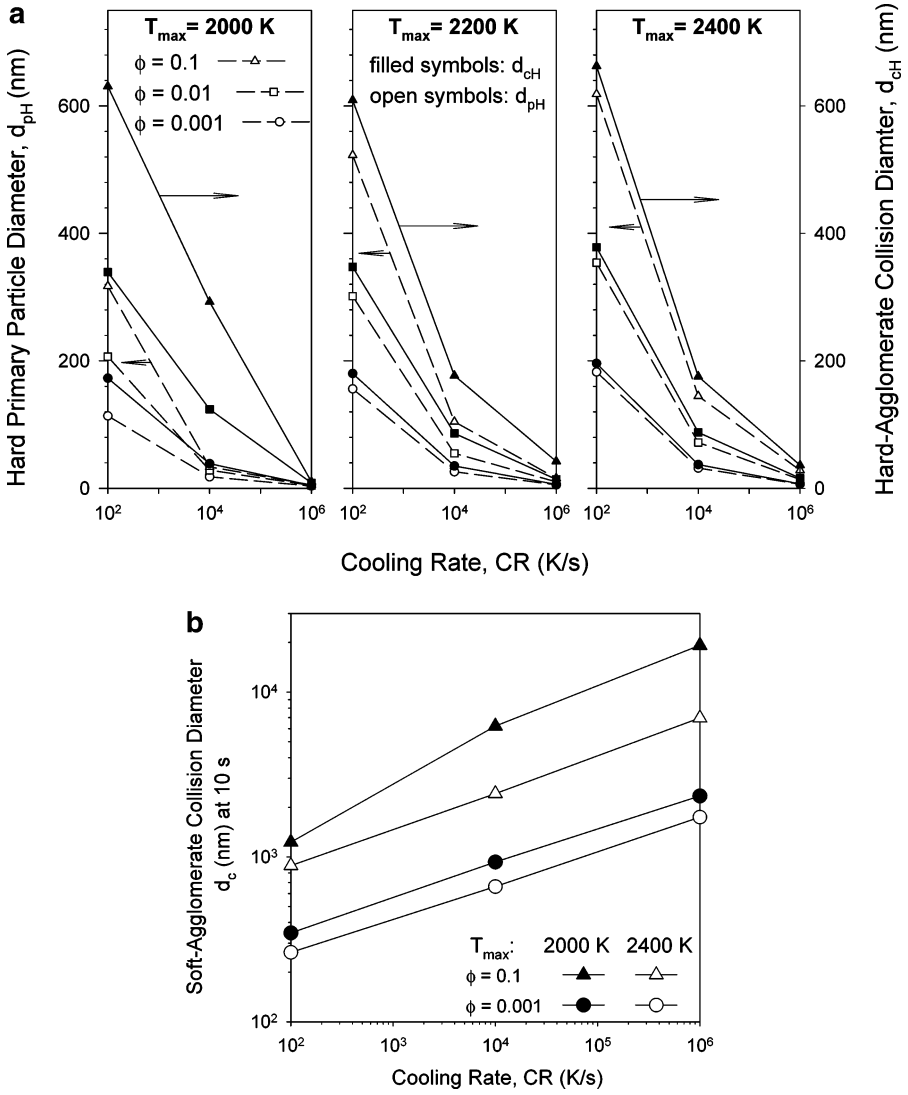

Figure 7. Silica: (a) hard-primary particle diameters (d_{pH}'s) (dashed lines and open symbols) and hard-agglomerate collision diameters (d_{cH}'s) (solid lines and filled symbols); (b) agglomerate collision diameters after 10 s as a function of the cooling rate (CR), maximum carrier gas temperature (T_{max}), and initial $SiCl_4$ molar fraction (ϕ) for $t_{max} = 2$ ms.

tration increases the particle concentration during the early full coalescence period, resulting in bigger primary particles. This is consistent with Pratsinis et al.,[2] who observed larger Brunauer−Emmett−Teller (BET) diameters by increasing the $TiCl_4$ inlet concentration during the flame synthesis of TiO_2 powders. This result is consistent also with Kammler et al.,[35] who produced bigger silica−carbon nanoparticles in a hydrogen diffusion flame by increasing the precursor (HMDSO) loading (feed). Likewise, higher particle concentrations increase agglomerate diameters.

Finally, the effect of extending the initial heating period (t_{max}) by up to a factor of 10 from its typical value (2 ms) is shown in Figure 6 for $T_{max} = 2400$ K, $\phi = 0.01$, and CR $= 10^6$ K/s. The t_{max} value affects essentially the period of full coalescence, as it prolongs the particle residence time at high temperatures. Hence, the impact of the initial heating time could be amplified at cooling rates high enough to quench particle evolution at its first steps (Figure 6). Here, a prolonged heating period followed by practically instant cooling favors synthesis of twice-as-large hard-primary particles and smaller soft agglomerates.

(35) Kammler, H. K.; Mueller, R.; Senn, O.; Pratsinis, S. E. *AIChE J.* **2001**, *47*, 1533.

Agglomeration Maps. Figure 7a shows the hard-primary (open symbols) and hard-agglomerate collision (filled symbols) particle diameters as a function of the cooling rate (CR) for $t_{max} = 2$ ms, three maximum carrier gas temperatures ($T_{max} = 2000$, 2200, and 2400 K), and three initial $SiCl_4$ molar fractions ($\phi = 0.1$ (triangles), 0.01 (squares), and 0.001 (circles)). Furthermore, Figure 7b shows the collision particle diameters after a residence time of 10 s for the same conditions as those in Figure 7a. Under all conditions, increasing the cooling rate decreases both the hard-primary and hard-agglomerate collision diameters (Figure 7a), while it increases the product soft-agglomerate collision diameter (Figure 7b). Likewise, increasing the $SiCl_4$ concentration (ϕ) increases all the particle diameters. For rapid cooling (most notably, for CR $= 10^6$ K/s), the difference between d_{cH} and d_{pH} can be small indicating rather spherical, nonagglomerated particles, as shown in Figure 3a. It should be noted also that at $T_{max} > 2400$ K only soft agglomerates of spherical particles are formed for the employed ϕ, t_{max}, and CR values. Moreover, the results for $t_{max} = 20$ ms (and $T_{max} > 2000$ K) are virtually the same with differences only at CR $= 10^6$ s, as discussed in Figure 6.

Irrespective of the cooling rate and the initial precursor molar fraction, the conversion of $SiCl_4$ is complete at the

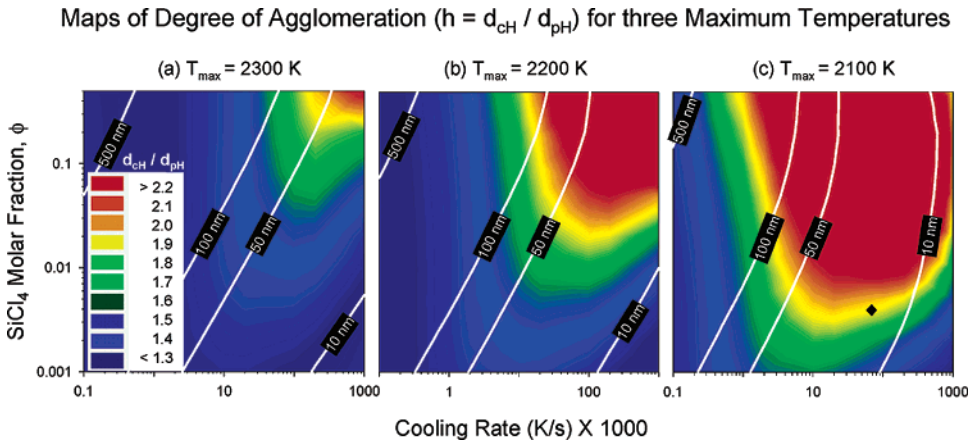

Figure 8. Mapping the degree of agglomeration ($h = d_{cH}/d_{pH}$) in the process parameter space of the inlet $SiCl_4$ molar fraction (ϕ) and cooling rate (CR, K/s) for $t_{max} = 2$ ms and (a) $T_{max} = 2300$ K, (b) $T_{max} = 2200$ K, and (c) $T_{max} = 2100$ K. Isopleths of the primary particle diameters (d_{pH}'s, nm) are shown also (white lines). Increasing T_{max} reduces the degree of agglomeration and increases the hard-primary particle diameter (d_{pH}) at even higher cooling rates. In part c, the data of Zhu and Pratsinis[8] (black diamond) are shown to be consistent with these maps.

end of the heating period ($t = t_{max}$) for $T_{max} \geq 2200$ K. This condition, however, is not satisfied at $T_{max} = 2000$ K. Thus, although a cooling rate of 10^4 K/s effectively slows sintering that results in similar (hard-) primary particle diameters regardless of the precursor concentrations for $T_{max} = 2000$ K (Figure 7a), the corresponding hard-agglomerate collision diameters (d_{cH}'s) are still very different. At $T_{max} = 2000$ K and CR $= 10^4$ K/s, the conversion of $SiCl_4$ is ~63% just after $t_{max} = 2$ ms and continues to completion (100%) after another 1.5 ms. For CR = 100 K/s, the temperature is high enough to facilitate sintering and permit fast completion of $SiCl_4$ oxidation (within <1 ms after $T_{max} = 2000$ K), while, at $T_{max} = 2000$ K and CR $= 10^6$ K/s, the temperature drops sharply enough to quickly freeze both the coalescence and reaction of the precursor (at ~85%), resulting in incomplete conversion or the so-called "chloride slip" from the reactor. Generally, if full conversion of the precursor and formation of rather nonagglomerated particles ($d_{cH}/d_{pH} < 2$) are sought, the maximum process temperature should be (here) larger than 2000 K or t_{max} must be increased. Moreover, if the desired product particle is relatively small (i.e., between 5 and 40 nm), high cooling rates should be employed (Figure 7a).

Figure 8 shows maps of the degree of agglomeration at the end of the hard-agglomerate region (in terms of d_{cH}/d_{pH}) in the process parameter space of the inlet $SiCl_4$ molar fraction (ϕ) and the cooling rate (CR, K/s) for (a) $T_{max} = 2300$ K, (b) $T_{max} = 2200$ K, and (c) $T_{max} = 2100$ K, for $t_{max} = 2$ ms. Isopleths (lines) of hard-primary particle diameters (d_{pH}'s, nm) are also superimposed on top of the corresponding contour plots. More specifically, the conditions of Figure 8c (black diamond) are close to those of Zhu and Pratsinis[8] regarding the synthesis of SiO_2 from $SiCl_4$ in a diffusion flame with oxygen as the main oxidant gas (thus achieving $T_{max} \approx 2100$ K). In fact, if fast mixing of the flame gases is assumed, the average CR is ~65 000 K/s, $\phi \approx 0.004$, and $t_{max} \approx 4$ ms. These conditions correspond here to a rather low degree of agglomeration ($h = 1.9$) consistent with their TEM data (Figure 8c, black diamond). At low process temperatures (in terms of T_{max}), degrees of agglomeration bigger than 2.2 (Figure 8, red) span over a wider region of cooling rates and precursor concentrations. Sintering places an upper limit to particle coalescence at a set d_p value (Figure 2a, solid line). As the maximum process temperature increases, sintering is enhanced, increasing that limiting d_p value, hence confining the regions of a high degree of agglomeration ($h > 2.2$) at high cooling rates and precursor concentrations (Figure 8a). Likewise, at higher T_{max} values, the isopleths of hard-primary particle diameters (d_{pH}'s) shift more to the right, as now larger primary particle sizes can be achieved even at higher cooling rates. In summary, the above analysis (Figure 8) could be used as a road map for the design of process conditions leading to product particles of special characteristics. Thus, for instance, if more flexibility is desired (i.e., the end product should have a specific size with a rather low degree of agglomeration), a high T_{max} value should be combined with selected cooling rates (Figure 8a).

Conclusions

The evolution of aerosol primary particle and agglomerate collision diameters was used here to distinguish periods (or regions) for synthesis of soft agglomerates (where constituent, primary particles are typically held together by rather weak van der Waals forces), hard agglomerates (where primary particles are held together by stronger sintering or chemical bonds), and even nonagglomerates by accounting for simultaneous gas phase chemical reaction, coagulation, and sintering of silica (SiO_2) nanoparticles by silicon tetrachloride ($SiCl_4$) oxidation, neglecting particle polydispersity. The onset of hard-agglomerate formation was defined when the agglomerate collision diameter was larger by 1% than that of the constituent primary particles. Likewise, soft agglomerates were formed when the primary particle diameter reached 99% of its final constant value. The process conditions (precursor initial volume fraction, maximum temperature, residence time, and cooling rate) promoting or suppressing the onset of hard or soft agglomeration were systematically explored. Increasing the cooling rate decreased hard-agglomerate collision and primary particle diameters but increased soft-agglomerate collision diameters. Softly or even nonagglomerated silica particles of ~5−40 nm in diameter were predicted for maximum process temperatures above 2000 K (after 2 ms) followed by high cooling rates (>10^4 K/s).

Acknowledgment. Support by the Swiss Commission for Technology and Innovation, TopNano21, Grant No. 5978.2TNS, is acknowledged, and the assistance of Robert Grass is appreciated. This paper received the best poster award of PARTEC 2004, International Congress of Particle Technology, March 16-18, 2004, Nuremberg, Germany.

LA036389W